CAUCHY: Jurnal Matematika Murni dan Aplikasi
Volume 10(1) (2025), Pages 117-132
p-ISSN: 2086-0382; e-ISSN: 2477-3344

On Local Antimagic b −Coloring and Its Application for Spatial Temporal Graph Neural Network Network Time Series Forecasting on Horizontal Farming

R. Sunder[1], Ika Hesti Agustin[2,3,*], Dafik[2,3], Ika Nur Maylisa[2], N. Mohanapriya[4], Marsidi[5]

[1]School of Computer Science and Engineering, Galgotias University, India
[2]PUI-PT Combinatorics and Graph, CGANT, University of Jember, Indonesia
[3]Department of Mathematics, University of Jember, Indonesia
[4]Department of Mathematics, Kongunadu Arts and Science College, Tamil Nadu, India
[5]Department of Mathematics Education, Universitas PGRI Argopuro Jember, Indonesia

Email: ikahesti.fmipa@unej.ac.id

ABSTRACT

This article discusses a local antimagic b −coloring which is a combination between antimagic labeling and b −coloring. We define a vertex weight of $v \in V$ as $w(v) = \Sigma_{e \epsilon E(v)} f(e)$ where $E(v)$ is the set of edges incident to v. The function f is referred to as a local antimagic labeling if, for any two adjacent vertices, their vertex weights are distinct. Additionally, a b −coloring of a graph is defined as a proper k −coloring of the vertices of G where each color class contains at least one vertex that has neighbors in all other $k-1$ color classes. If we assign colors to vertices based on their vertex weights $w(v)$ such that the resulting graph coloring satisfies the b −coloring property, this is referred to as a local antimagic b −coloring of graphs. The local antimagic b −chromatic number, denoted $\varphi_{la}(G)$, represents the maximum number of colors achievable through any local antimagic b −coloring of G. This paper aims to introduce and explore new lemmas and theorems concerning $\varphi_{la}(G)$. Moreover, to demonstrate the practical application of local antimagic b −coloring, the paper concludes with an analysis of its implementation in Graph Neural Networks (GNN) for multi-step time series forecasting of NPK (Nitrogen, Phosphorus, and Potassium) concentrations in companion plantations. The findings highlight the utility of this method in determining optimal planting layouts and fertilizer application schedules, enhancing precision and sustainability in agriculture. Simplified explanations ensure accessibility to a broader audience.

Keywords: Local antimagic b −coloring, STGNN, time series forecasting, NPK, precision agriculture.

INTRODUCTION

All graphs, in this study, are simple, connected, and undirected graph. For a bijection $f: E(G) \rightarrow \{1,2,3,\ldots,|E(G)|\}$. Arumugam *et. al.* defined local vertex antimagic labeling if for every two adjacent vertices u and v, their vertex weight $w(u) \neq w(v)$

Submitted: November 22, 2024 Reviewed: December 11, 2024 Accepted: January 22, 2025
DOI: http://dx.doi.org/10.18860/ca.v10i1.29968

where $w(u) = \sum_{e\epsilon\, E(u)} f(e)$, see [1]. If each vertex is assigned a color based on its vertex weight $w(v)$ such that no two adjacent vertices share the same color, this is referred to as a local antimagic coloring. The local antimagic chromatic number, denoted as $\chi_{la}(G)$, represents the minimum number of colors required across all possible local antimagic labelings of G. Read some new results of $\chi_{la}(G)$ in G [2]-[6].

Next, the researchers study the concept of b −coloring. It is a proper k −coloring of G such that in each color class there exists a vertex having neighbors in all other $k-1$ color classes. The b −chromatic number of a graph G, denoted as $\varphi(G)$, is the largest k for which G has b −coloring by k −colors. It is easy to understand that $\chi(G) \leq \varphi(G)$. Some new results for b −coloring can be referred to Jakovac and Klavzar [7] who obtained b −chromatic number of cubic graphs. Irving and Manlove [8] found b −chromatic number of trees. Javadi and Omoomi [9, 10] determined b −chromatic number of Kneser graphs and the cartesian product of paths and cycles with complete graphs and the cartesian product of two complete graphs. Kok and Sudev [11] determined the b −chromatic number of linear Jaco graph, Ornated graph, Rasta graph, Chithra family graphs, and set graph. Diego and Gella [12] found the b −chromatic number of the center graph, middle graph, and total graph of the bistar graph. The other results regarding b −coloring can be seen in [13]-[21].

Combining the aforementioned concepts, we propose a new idea called local antimagic b −coloring. Consider a mapping $f: E(G) \rightarrow \{1,2,3,\ldots,|E(G)|\}$. For a vertex $v \in V$, its weight is defined as $w(v) = \Sigma_{e\epsilon\, E(v)} f(e)$, where $E(v)$ represents the set of edges incident to v. The mapping f is described as a local antimagic labeling if the vertex weights of any two adjacent vertices are distinct. Additionally, a b −coloring of a graph refers to a valid k −coloring of the vertices of G such that at least one vertex in each color class is adjacent to vertices in all other $k-1$ color classes. If vertices are colored based on their vertex weights $w(v)$ in a manner that ensures proper graph coloring satisfying the conditions of b −coloring, this concept is termed local antimagic b −coloring of graphs.

Furthermore, companion plants are plants that are grown together in a garden or agricultural setting because they are believed to have mutually beneficial effects on each other. These benefits can include pest control, improved growth, and enhanced flavor. Companion planting can play a role in fulfilling supply and demand in agriculture. By strategically choosing companion plants, farmers can optimize their yields, reduce the need for synthetic inputs, and enhance the overall sustainability of their agricultural practices. Some research on companion planting can be seen in [22]-[26]. The application of local antimagic b −coloring on companion farming is indeed relevant, since in this concept we obtain the largest number of colors instead of the smallest one. Thus, in this type of farming, we can maximize the type of agricultural yields.

Moreover, Graph Neural Networks (GNN) are a class of machine learning models designed to operate on graph-structured data [27-29]. Graphs consist of vertices connected by edges, and they are a natural way to represent relationships and interactions in various domains such as social networks, biological systems, recommendation systems, and including the planting layout in precision agriculture [30-31]. GNN can be utilized for time series forecasting in agriculture to model the spatial and temporal interdependencies present in agricultural datasets [32-34]. Representing agricultural fields as vertices in a graph, with edges representing spatial relationships, enables the model to capture dependencies between neighboring fields. This is particularly useful in precision agriculture where the conditions in one field may influence adjacent fields. GNN can learn spatial patterns and relationships among

different regions or crops, helping to identify how the conditions of one area may affect others.

This research investigate to explore novel lemmas and theorems associated with $\varphi_{la}(G)$. To demonstrate the practical utility of local antimagic $b-$coloring, we will conclude by analyzing its application in Graph Neural Networks (GNN) for multi-step time series forecasting of Nitrogen, Phosphorus, and Potassium (NPK) concentrations in companion plantations within precision agriculture.

METHODS

This research incorporates both analytical and experimental methodologies. The analytical method involves the application of a mathematical deductive framework to formulate various theorems. By leveraging established lower bounds, the study extends these foundations to generate novel theoretical insights.

Observation 2.1. [35] For any graph G, $\chi_{lea}(G) \geq \chi(G)$, where $\chi(G)$ is a chromatic number of graph coloring G.

.In the experimental method, computer programming will be utilized to simulate the development of autonomous Controlled Environment Agriculture (CEA) through multi-step time series forecasting of NPK concentrations for companion plantations, including Rosa sp., Bougainvillea spectabilis, Cryptanthus spp., and Bromeliaceae. Initially, the vertex embedding process of a single-layer Graph Neural Network (GNN) will be demonstrated using three feature datasets—Nitrogen (N), Phosphorus (P), and Potassium (K)—collected over a three-month observation period. Subsequently, a Spatial Temporal Graph Neural Network (STGNN) program will be implemented to train a model using 80% of the data from the vertex embedding process, test its performance, and forecast NPK fertilization schedules to determine optimal fertilization timing for Rosa sp., Bromeliaceae, Bougainvillea spectabilis, and Cryptanthus spp. plantations. The algorithm incorporates the study of fuel purchase distribution using STGNN in conjunction with local antimagic $b-$coloring.

GNN Algorithm with a Single Layer

Input	Graph data $G(V,E)$, matrix adjacency A from graph G, matrix feature $H_{n\times m}$, and tolerance ϵ.
Output	Forecasting results.
Procedure 1	Initialize weights W, bias β, learning rate α. *for* $error < \epsilon$ *do* Message passing $m_u^l = MSG^l(h_u^{l-1})$ Aggregate the message $h_v^l = AGG^l\{m_u^{l-1}, u \in N(v)\}$ Determine the $error^l = \frac{\|h_{v_i} - h_{v_i}\|_2}{\|E\|}$ Update the learning weight $W^{l+1} = W_j^l + \alpha \times z_j \times e^l$ *end*
Procedure 2	Save embedding results into a vector.
Procedure 3	Load the embedding data.mat.
Procedure 4	Use time series forecasting to do forecasting.
Procedure 5	Have the best training, testing and forecasting results.

The algorithm can be simply represented in the form of a flowchart as follows.

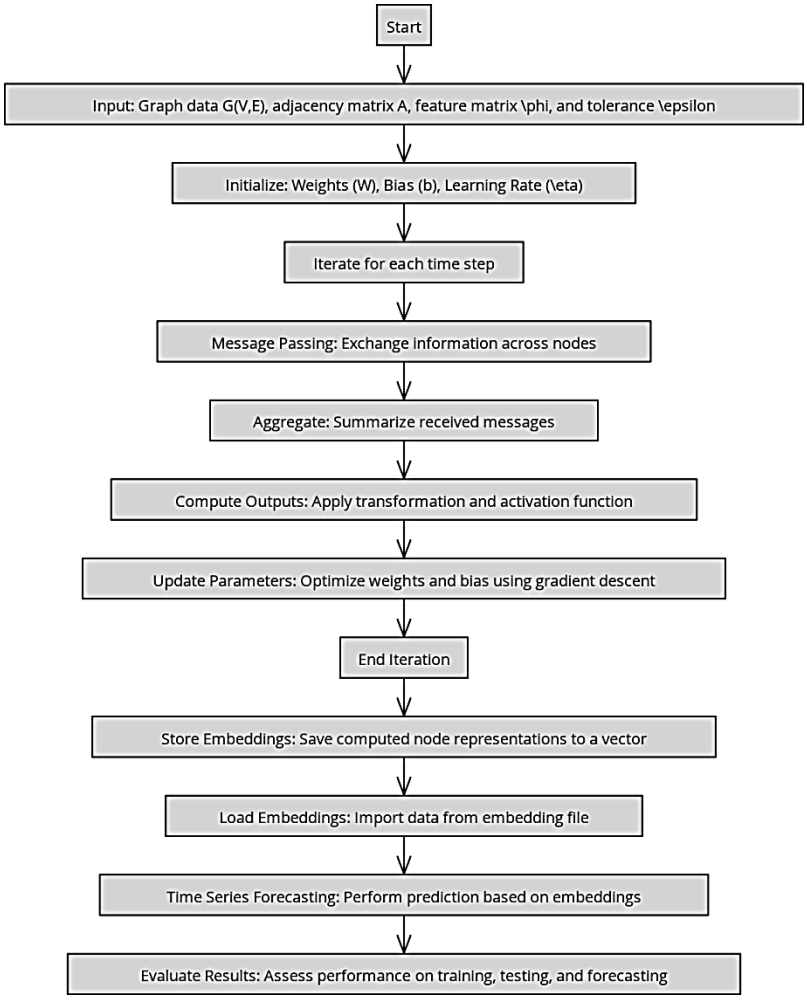

Figure 1. Flowchart for the GNN algorithm.

RESULTS AND DISCUSSION

In this section we present the results into four subsections, namely: local antimagic $b-$coloring; data setup; numerical analysis; and performance of STGNN training and testing. Although divided into several sub-sections, we have thoroughly explained the interconnections between each of these sub-sections.

Local Antimagic $b-$Coloring

This subsection contains new theorems on the topic of local antimagic $b-$coloring. There are two new theorems, with one of them chosen by the researcher as a design for planting topology in companion planting. The following are the theorems with their proofs.

Theorem 2.1. Let B_n be a book graph, for $n \geq 3$ the local antimagic $b-$chromatic number of B_n is 4.

Proof. Let B_n be a cycle graph with vertex set $V = \{a, b, u_i, v_i : 1 \leq i \leq n\}$ and edge set $E = \{ab, au_i, bv_i, u_iv_i : 1 \leq i \leq n\}$. Since $\chi_{la}(B_n) = 4$, such that $\varphi_{la}(B_n) \geq \chi_{la}(B_n) = 4$.

Furthermore to show $\varphi_{la}(B_n) \leq 4$, we construct the edge labels on B_n as follows. We divide into cases, namely for even n and odd n.

Case 1. For even n

$$f(au_i) = \begin{cases} i, & if\ 1 \leq i \leq \frac{n}{2}+1 \\ n+i, & if\ \frac{n}{2}+2 \leq i \leq n \end{cases} \qquad f(bv_i) = \begin{cases} n+i, & if\ 1 \leq i \leq \frac{n}{2}+1 \\ i, & if\ \frac{n}{2}+2 \leq i \leq n \end{cases}$$

$$f(u_iv_i) = 3n+1-i, if\ 1 \leq i \leq n \qquad f(ab) = 3n+1$$

Using the edge labeling above, we can determine the vertex weight of each vertex on B_n. We can determine the number of different vertex weights. Therefore, we can obtain the number of different vertex weights as follows.

$$w(u_i) = \begin{cases} 3n+1, if\ 1 \leq i \leq \frac{n}{2}+1 \\ 4n+1, if\ \frac{n}{2}+2 \leq i \leq n \end{cases} \qquad w(v_i) = \begin{cases} 4n+1, if\ 1 \leq i \leq \frac{n}{2}+1 \\ 3n+1, if\ \frac{n}{2}+2 \leq i \leq n \end{cases}$$

$$w(a) = n^2 + \frac{5n}{2} + 1 \qquad w(b) = \frac{15n^2}{8} + \frac{5n}{4}$$

Case 2. For odd n

$$f(au_i) = \begin{cases} i, if\ 1 \leq i \leq \lceil \frac{n}{2} \rceil \\ n+i, if\ \lceil \frac{n}{2} \rceil + 1 \leq i \leq n \end{cases} \qquad f(bv_i) = \begin{cases} n+i, if\ 1 \leq i \leq \lceil \frac{n}{2} \rceil \\ i, \quad if\ \lceil \frac{n}{2} \rceil + 1 \leq i \leq n \end{cases}$$

$$f(u_iv_i) = 3n+1-i, if\ 1 \leq i \leq n \qquad f(ab) = 3n+1$$

Using the edge labeling above, we can determine the vertex weight of each vertex on B_n. We can determine the number of different vertex weights. Therefore, we can obtain the number of different vertex weights as follows.

$$w(u_i) = \begin{cases} 3n+1, if\ 1 \leq i \leq \frac{n}{2}+1 \\ 4n+1, if\ \frac{n}{2}+2 \leq i \leq n \end{cases} \qquad w(v_i) = \begin{cases} 4n+1, if\ 1 \leq i \leq \frac{n}{2}+1 \\ 3n+1, if\ \frac{n}{2}+2 \leq i \leq n \end{cases}$$

$$w(a) = n^2 + 3n + 1 \qquad w(b) = n^2 + 4n + 1$$

In the local antimagic b −coloring concept, the color on each vertex is induced from the vertex weight. From the vertex weights, We know that there are four colors such that it means $\varphi_{la}(B_n) \leq 4$. Since we have $\varphi_{la}(B_n) \geq 4$ and $\varphi_{la}(B_n) \leq 4$, it concludes that $\varphi_{la}(B_n) = 4$. □

For example, an illustration of local antimagic b −coloring on graph B_5 is presented in Figure 2.

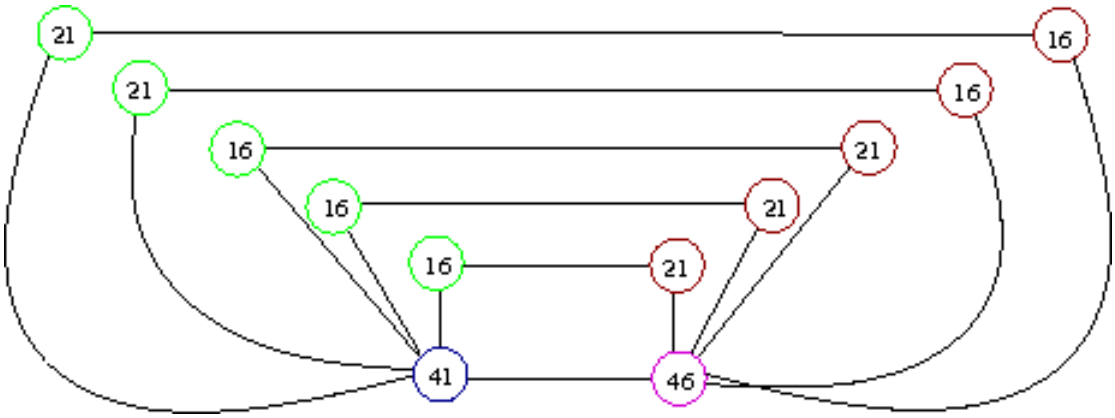

Figure 2. Local antimagic b −coloring on graph B_5.

Data Setup

In this subsection we will explain the process of applying local antimagic b −coloring to companion planting. The next step is to perform time series forecasting on the dataset obtained from observations of plants on companion planting. The data is in the form of nitrogen, phosphorus and potassium data monitored by NPK sensors placed on each representative plant. The placement of the NPK sensor is adapted to the local antimagic b −chromatic number value of the graph we have chosen.

In this study, the chromatic number of the graph represents the variety of plants on the companion planting. The chromatic number is derived from the number of color classes in the graph. For example, in the graph B_n, where $n \geq 3$, the value of $\varphi_{la}(B_n) = 4$. In this study we choose B_8 as an example. The graph B_8 consists of 18 vertices. In detail, the coloring of the graph B_8 can be seen in Figure 3.

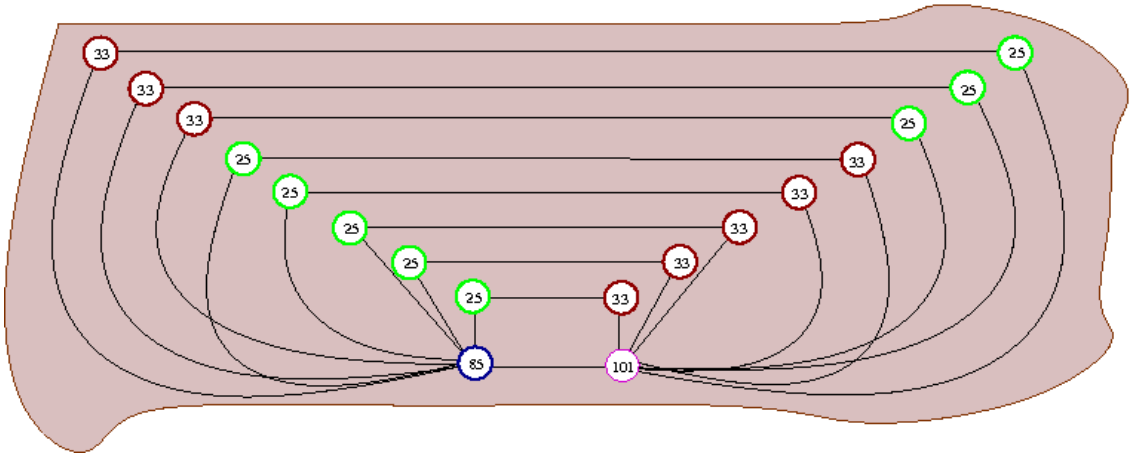

Figure 3. Local antimagic b −coloring on graph B_8 as planting topology design in companion planting.

Figure 3 shows that there are four color classes in the book graph, namely color classes 25, 33, 85 and 101. The figure also shows that color class 25 neighbors color classes 33, 85 and 101. Color class 33 neighbors color classes 25, 85 and 101. Color class 85 neighbors color classes 25, 33 and 101. In addition, color class 101 neighbors color classes 25, 33 and 85. Color class 25 represents watermelon plants, color class 33 represents pumpkin plants, color class 85 represents melon plants, while color class 101 represents cantaloupe plants. This shows that there are four types of plants in companion planting design which match with local antimagic b −coloring concept on graph B_n as shown in Figure 4. In order to predict the fertilization time, we also installed NPK sensors on the representatives of each of the four plants. The observation period is

90 days. With the prediction results from the time series prediction using GNN, the fertilization time to increase the decreasing NPK levels can be done in time. As a result, the productivity of this companion planting is more optimal.

Figure 4. Planting design for companion planting based on local antimagic b −coloring on graph B_8.

Numerical Analysis

In this subsection, we will present and explain the results in the following manner. Initially, we provide an analytical explanation of the embedding process for the feature nodes and the local antimagic b −coloring of the given graph. Subsequently, we utilize the NPK data to derive the STGNN model, which is then applied to forecast optimal plant fertilization timings in the context of companion planting..

Observation 3.1. Given that a graph G of order n. Suppose that vertex and edge sets are $V(G) = \{v_1, v_2, v_3, \dots, v_{n-1}, v_n\}$ and $E(G) = \{v_i v_j | v_i, v_j \in V(G)\}$, respectively. Given that vertex features as follows $h_{v_i} = \begin{bmatrix} a_{1,1}\ a_{1,2}\ a_{1,3}\ \dots\ a_{1,m}\ a_{2,1}\ a_{2,2}\ a_{2,3}\ \dots\ a_{2,m}\ \vdots\ a_{n,1}\ \vdots\ a_{n,2}\ \vdots\ a_{n,3}\ \ddots\ \dots\ \vdots\ a_{n,m} \end{bmatrix}$. The vertex embedding can be determined using the messages passing from vertex v's neighbors $h_v^{l+1} = AGG\{m_u^{l+1}, u \in N(v)\}$ under the aggregation **sum**$(\cdot)$, where $l = 0,1,2,3, \dots, k$. Thus $h_v^{l+1} = SUM\{m_u^{l+1}, u \in N(v)\}$ in regards to the matrix $B = A + I$ where A, I are adjacency and identity matrix, respectively.

Proof. From the graph G, the adjacency matrix A can be obtained. To account for the self-adjacency of each vertex in G, the identity matrix I is added to A, producing the matrix B as shown.

$$B = A + I = \begin{bmatrix} b_{1,1}\ b_{1,2}\ b_{1,3}\ \dots\ b_{1,n}\ b_{2,1}\ b_{2,2}\ b_{2,3}\ \dots\ b_{2,n}\ \vdots\ b_{n,1}\ \vdots\ b_{n,2}\ \vdots\ b_{n,3}\ \ddots\ \dots \\ \vdots\ b_{n,n}\ \end{bmatrix}$$

Based on the single-layer GNN algorithm, the initialization of the learning weight matrix should be performed as follows.

$$W = \begin{bmatrix} w_{1,1}\ w_{1,2}\ w_{1,3}\ \dots\ w_{1,m}\ w_{2,1}\ w_{2,2}\ w_{2,3}\ \dots\ w_{2,m}\ \vdots\ w_{n,1}\ \vdots\ w_{n,2}\ \vdots\ w_{n,3}\ \ddots\ \dots \\ \vdots\ w_{n,m} \end{bmatrix}$$

This weight is utilized to calculate m_{v_i} and subsequently update the weight for the next iteration. The vertex embedding process in GNN is divided into two phases: message passing and aggregation. During the first phase, message passing is performed $m_u = MSG(h_u)$. For linear layer we have $m_u^{l+1} = W^l \cdot h_u^l$, where $l = 0,1,2,3, \dots k$. We can iteratively start the calculation as follows:

$$\begin{aligned} m_{v_i}^l &= H_{v_i}^0 \cdot W^0 \\ &= \begin{bmatrix} a_{1,1}\ a_{1,2}\ a_{1,3}\ \dots\ a_{1,m}\ a_{2,1}\ a_{2,2}\ a_{2,3}\ \dots\ a_{2,m}\ \vdots\ a_{n,1}\ \vdots\ a_{n,2}\ \vdots\ a_{n,3}\ \ddots\ \dots \\ \vdots\ a_{n,m} \end{bmatrix} \\ &\quad \times \begin{bmatrix} w_{1,1}\ w_{1,2}\ w_{1,3}\ \dots\ w_{1,m}\ w_{2,1}\ w_{2,2}\ w_{2,3}\ \dots\ w_{2,m}\ \vdots\ w_{n,1}\ \vdots\ w_{n,2}\ \vdots\ w_{n,3} \\ \ddots\ \dots\ \vdots\ w_{n,m} \end{bmatrix} \\ &= \begin{bmatrix} a_{1,1} \times w_{1,1} + \dots + a_{1,m} \times w_{m,1}\ a_{2,1} \times w_{1,1} + \dots + a_{2,m} \times w_{m,1}\ a_{1,1} \times w_{1,2} + \dots + a_{1,m} \\ \times w_{m,2}\ a_{2,1} \times w_{1,2} + \dots + a_{2,m} \times w_{m,2}\ \dots\ \dots\ a_{1,1} \times w_{1,m} + \dots + a_{1,m} \\ \times w_{m,m}\ a_{2,1} \times w_{1,m} + \dots + a_{2,m} \times w_{m,m}\ \vdots\ a_{n,1} \times w_{1,1} + \dots + a_{n,m} \times w_{m,1} \\ \vdots\ a_{n,1} \times w_{1,2} + \dots + a_{n,m} \times w_{m,2}\ \ddots\ \dots\ \vdots\ a_{n,1} \times w_{m,1} + \dots + a_{n,m} \times w_{m,m} \end{bmatrix} \end{aligned}$$

Once the above process has been done we do the second step, namely aggregation in regards with v's neighbors. By applying the aggregation **sum**$(\cdot)$, for $h_v^{l+1} = AGG\{m_u^{l+1}, u \in N(v)\}$ we have $h_v^{l+1} = SUM\{m_u^{l+1}, u \in N(v)\}$ in regards with matrix $B = A + I$, the embedding vector $h_{v_i}^1$ can be written as follows.

After completing the aforementioned process, the next step is to perform aggregation concerning v's neighbors. By applying the aggregation function **sum**$(\cdot)$, where $h_v^{l+1} = AGG\{m_u^{l+1}, u \in N(v)\}$, this can be expressed as $h_v^{l+1} = SUM\{m_u^{l+1}, u \in N(v)\}$. Considering the matrix $B = A + I$, the embedding vector $h_{v_i}^1$ can be represented as follows.

$$h_{v_i}^{l+1} = \begin{bmatrix} m_{v_{1,1}}^{l+1}\ m_{v_{1,2}}^{l+1}\ m_{v_{1,3}}^{l+1}\ \dots\ m_{v_{1,m}}^{l+1}\ m_{v_{2,1}}^{l+1}\ m_{v_{2,2}}^{l+1}\ m_{v_{2,3}}^{l+1}\ \dots\ m_{v_{2,m}}^{l+1}\ \vdots\ m_{v_{n,1}}^{l+1}\ \vdots\ m_{v_{n,2}}^{l+1}\ \vdots\ m_{v_{n,3}}^{l+1} \\ \ddots\ \dots\ \vdots\ m_{v_{n,m}}^{l+1} \end{bmatrix}$$

To continue, it is essential to compute the error value, which indicates the closeness of two neighboring vertices in the embedding space. A lower error value signifies a shorter distance between these vertices. The error is defined as follows: $error^l = \frac{\left\| h_{v_i} - h_{v_j} \right\|_{inf}}{|E(G)|}$ where $i, j \in \{1,2,\dots,n\}$. We need to check whether $error \leq \epsilon$. If no, we need to update new W^l using the obtained $h_{v_i}^l$ in the previous iteration. We update the learning weight matrix by using $W^{l+1} = W^l + \alpha \times error^l \times \left(h_{v_i}^l\right)^T \times h_{v_i}^{l+1}$ until $error \leq \epsilon$.

We must verify if the error is less than or equal to ϵ. If it is not, the weight matrix W^l needs to be updated using the previously calculated $h_{v_i}^l$ from the last iteration. The update is performed by applying the formula $W^{l+1} = W^l + \alpha \times error^l \times \left(h_{v_i}^l\right)^T \times h_{v_i}^{l+1}$, and this process continues until the condition $error \leq \epsilon$ is satisfied.

Performance of the STGNN Training and Testing

Applying the single layer GNN algorithm presented in the method section, we can develop and run a program to analyze the fertilization time of all plants in our companion planting. Fertilization is done to increase the NPK level which is decreasing day by day so that when the NPK level is minimal and fertilization is done, the NPK level returns to normal. The first step we do is collect some data from all types of plants regarding three features, namely Nitrogen, Phosphorus and Potassium levels within 90 days of observation. Once the NPK level data has been obtained, STGNN programming is developed to train 60% of the input data. Subsequently, the testing process is conducted using the remaining 40% of the input data. For the last step, we can estimate the fertilization time for the four plants. Figure 5 shows the data distribution over 90 days of observation time.

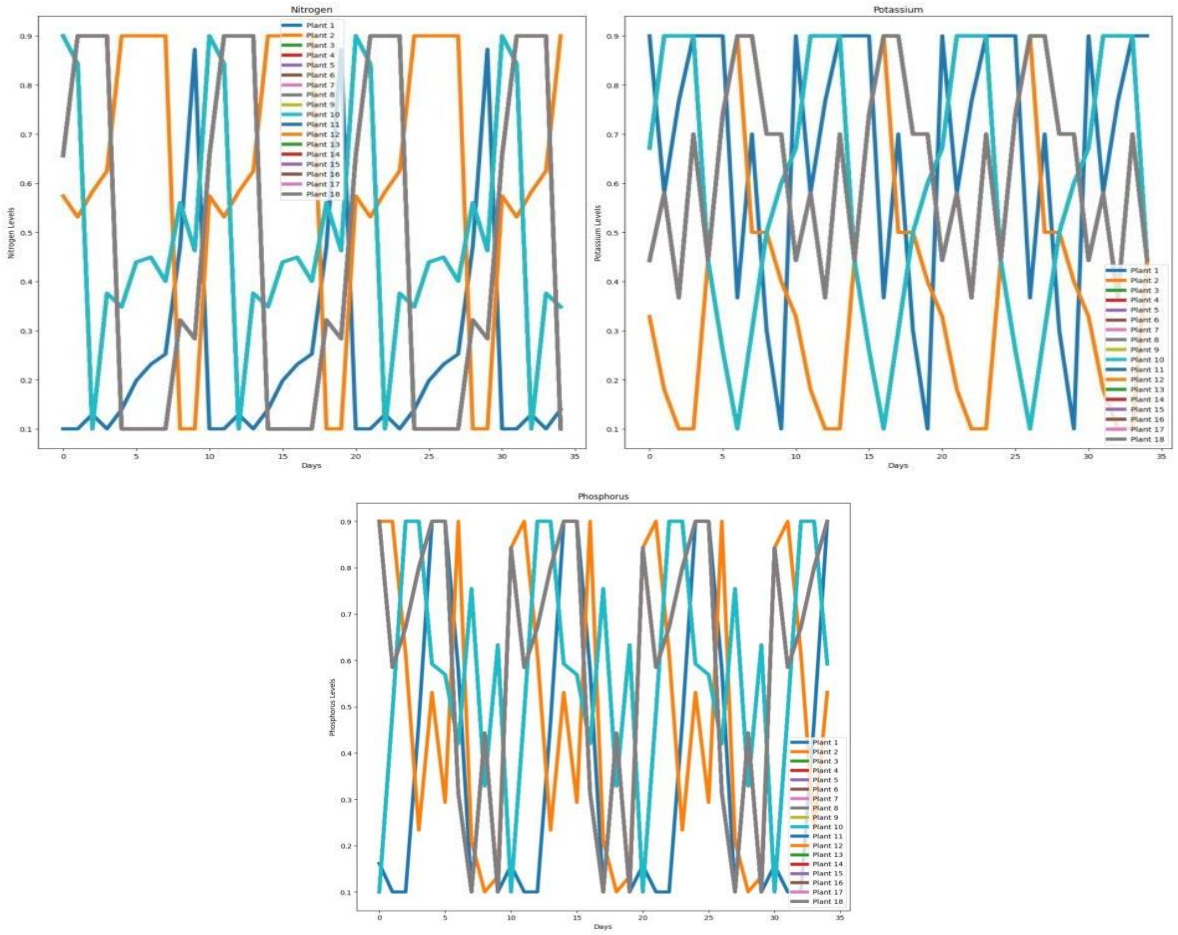

Figure 5. Distribusi of NPK data at 90 days of observation.

To describe the single-layer GNN algorithm, it is essential to establish the graph embedding for the four plant varieties. Each plant, represented as a vertex within the graph, is assumed to influence other plants if they are adjacent. Consequently, a message-passing process is implemented, taking into account the adjacency matrix for all plants in the companion planting scenario. Subsequently, we constructed an STGNN model for multi-step time series forecasting, utilizing 60% of the input data for training purposes. The training phase yielded a model, from which the one with the smallest error value was selected. Subsequently, the remaining 40% of the input data was used

for testing to determine the smallest Root Mean Square Error (RMSE) or Mean Square Error (MSE). The results of the testing process for plant x_1 are depicted in Figure 6.

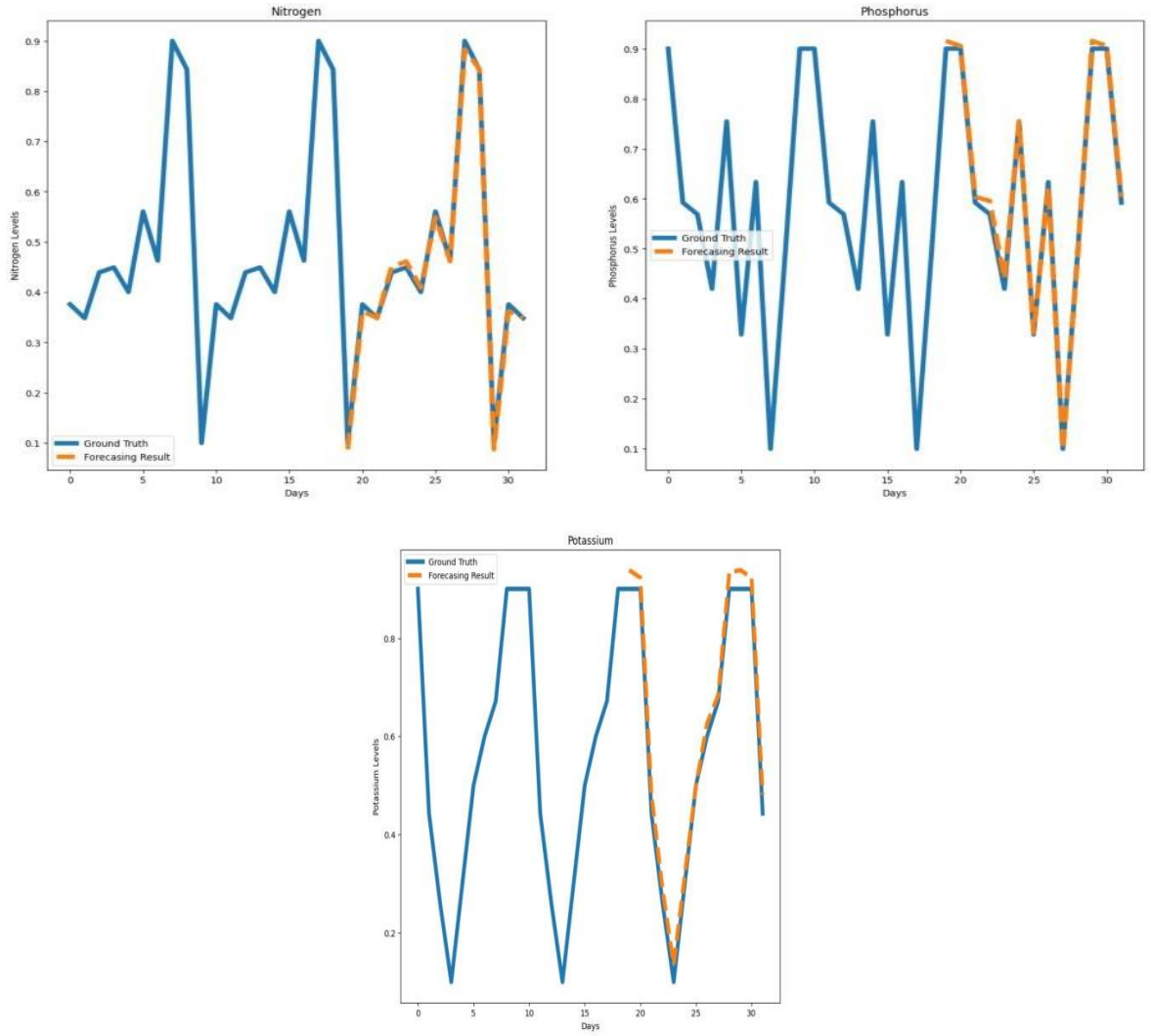

Figure 6. Results from testing the NPK levels data.

To validate the robustness of the STGNN model, six models were compared: Historical Average (HA), Auto Regressive Integrated Moving Average (ARIMA), Support Vector Regression (SVR), Graph Convolutional Networks (GCN), Gated Recurrent Unit (GRU), and Spatial Temporal Graph Neural Networks (STGNN). The results indicate that the STGNN model outperforms the others. As depicted in Figure 7, the STGNN model achieves the lowest error value after 200 epochs. Additionally, the RMSE values for the STGNN model are the smallest across both Dataset-1 and Dataset-2. Moreover, the graph in Figure 7 demonstrates that the STGNN model exhibits minimal fluctuations compared to the other models, further supporting its superior performance.

The comparison of the six models was evaluated using parameters such as RMSE, MAE, accuracy, and R^2, based on time series forecasting over the next 10, 20, 30, and 40 days. These comparison results are summarized in Table 1. From the table, it is evident that the STGNN model yields the lowest RMSE and MAE values compared to the other models, indicating that it has the smallest error. Consequently, the STGNN model is identified as the most accurate. Additionally, the STGNN model achieves the highest accuracy and R^2 values, further reinforcing its superiority among the six models.

Therefore, the STGNN model is deemed suitable for forecasting and monitoring fertilization schedules for the four plant varieties in the companion planting system. Figure 8 illustrates the results of multi-step time series forecasting for crop x_1.

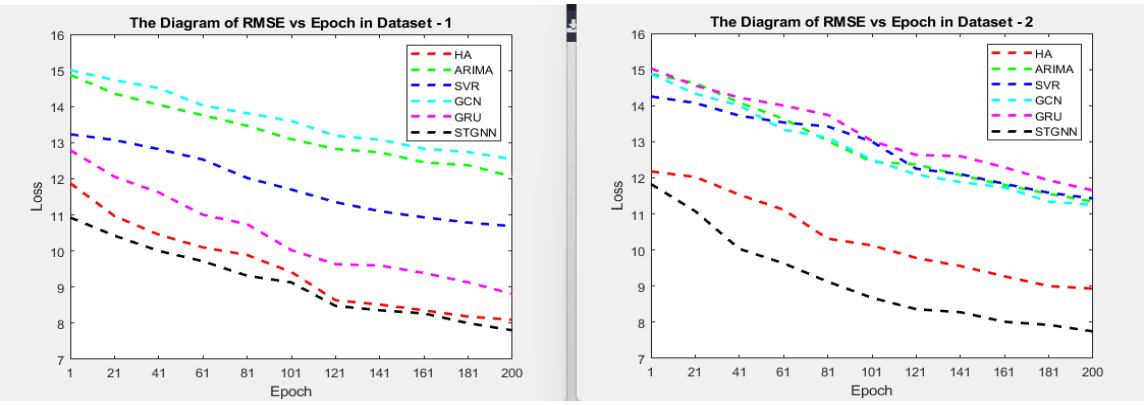

Figure 7. RMSE Value on Dataset-1 and Dataset-2.

Table 1. The outcomes of the predictions made by the STGNN model, along with those from other baseline approaches, on the dataset.

T	Matric	Dataset of NPK Levels in Four Plant Varieties					
		HA	**ARIMA**	**SVR**	**GCN**	**GRU**	**STGNN**
10 Days	RMSE	11.8770	14.8773	13.2317	15.0073	12.7911	10.9271
	MAE	9.9291	12.8572	11.0732	13.7322	10.6533	8.0097
	Accuracy	0.1782	0.3216	0.6461	0.5419	0.4053	0.8197
	R^2	0.3819	0.1725	0.5099	0.5099	0.2428	0.9726
20 Days	RMSE	10.9658	14.3578	13.0731	14.7306	12.0531	10.0231
	MAE	8.8535	12.0486	11.8201	12.5102	10.6217	8.0017
	Accuracy	0.2707	0.4278	0.4979	0.6305	0.1149	0.8564
	R^2	0.1818	0.3717	0.4129	0.5070	0.6351	0.8402
30 Days	RMSE	10.0989	13.7582	12.5321	14.0302	11.0021	9.7171
	MAE	8.8884	11.4666	10.0221	12.8132	9.7415	7.3146
	Accuracy	0.5694	0.7250	0.6961	0.5360	0.3024	0.8432
	R^2	0.8811	0.4819	0.6121	0.5017	0.7332	0.9490
40 Days	RMSE	9.4163	13.0954	11.7017	13.5991	10.0221	9.1287
	MAE	7.6342	11.8248	9.3517	11.1912	8.6331	7.4799
	Accuracy	0.2694	0.5267	0.6969	0.0242	0.3005	0.7218
	R^2	0.7810	0.6801	0.5132	0.4873	0.5427	0.9798

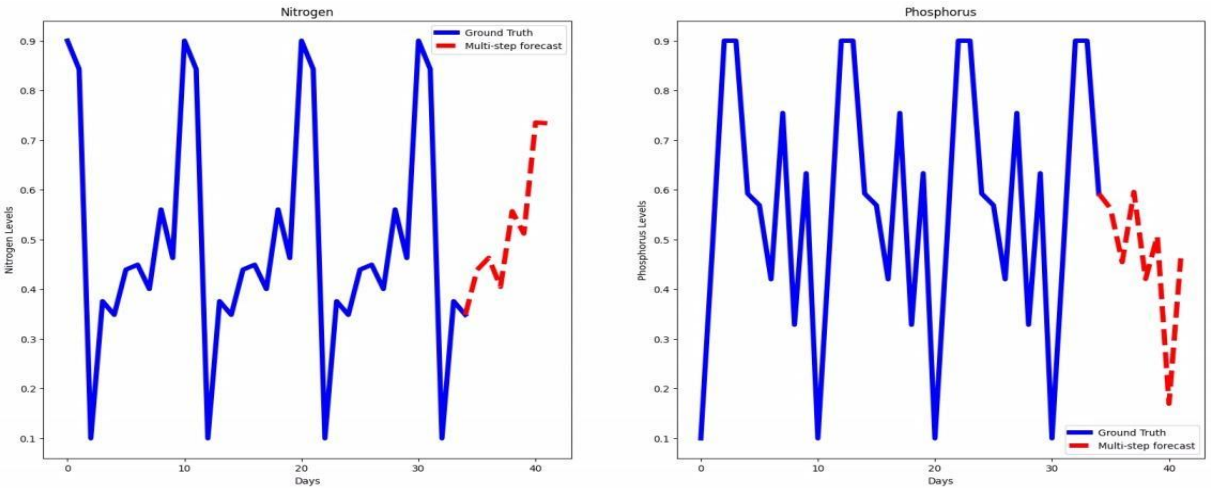

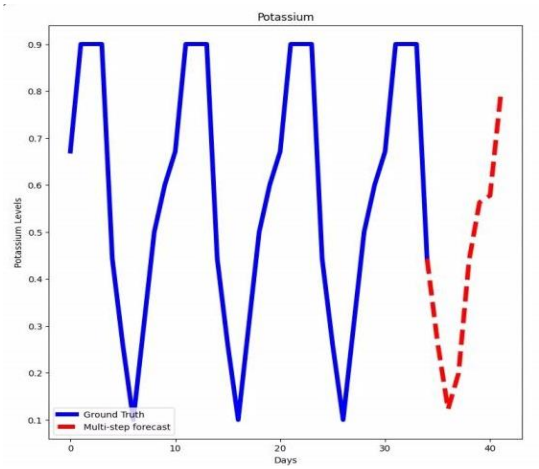

Figure 8. The distribution of NPK levels at the forecasting step

Discussion

This chapter will present and analyze the findings obtained from the conducted research. The results of this study show that the implementation of local antimagic b −coloring in planting topology design on companion planting is effective. This is evidenced by the increase in plant varieties in the planting topology design of the companion planting, so that the farming products are more optimal. In addition, based on time series forecasting through GNN that has been done, it is also known the right fertilization time for all plants on the companion planting.

Therefore, it can be said that this research contributes to two important areas, namely local antimagic b −coloring and time series forecasting using GNN. We build upon existing literature demonstrating that the concept of local antimagic b −coloring focuses on identifying the maximum chromatic value, which is subsequently utilized in designing crop patterns for companion planting. Some previous research related to this field can be found in [36-39]. In addition, this research also enriches the literature related to time series forecasting using GNN integrated with local antimagic b −coloring. Some previous research related to this field can be found in [40-42].

In exploring the integration of local antimagic b-coloring and time series forecasting using GNN, this study also draws upon foundational works in related graph coloring topics. [43] discussed rainbow antimagic coloring in special graphs, providing insights into antimagic properties that can inform chromatic evaluations. Similarly, [44] investigated the resolving numbers of special graphs, which further complements the theoretical underpinnings of graph operations and their applications. [45] explored the graceful chromatic number of unicyclic graphs, showcasing advanced graph coloring techniques that align with the innovative approaches proposed in this research. These works collectively strengthen the theoretical foundation of our study.

This research also has several strengths. First, we combine two different topics, namely local antimagic b −coloring and time series forecasting using GNN to create an innovative approach. Second, we conducted a series of careful experiments to test the performance of our method. However, this research also has limitations. We need further research in optimizing the parameters of local antimagic b −coloring and time series forecasting using GNN for special cases. Also, this approach requires special attention in data selection and preparation which can be a complicated task for future researchers.

CONCLUSIONS

This research contributes significantly to both theoretical advancements and practical applications in the fields of local antimagic $\boldsymbol{b}-$coloring and precision agriculture. The theoretical contributions include the development of a new theorem, namely $\boldsymbol{\chi_{la}(B_n) = 4}$ which provide novel insights into graph coloring applications. These results are utilized to design a planting topology for companion planting with four crop varieties: watermelon, melon, pumpkin, and cantaloupe. This choice reflects the compatibility of local antimagic $\boldsymbol{b}-$coloring with the companion planting concept, emphasizing its potential to optimize crop diversity and yield.

From a practical perspective, the integration of local antimagic $\boldsymbol{b}-$coloring with graph neural networks (GNN) for time series forecasting offers a robust approach to precision agriculture. The methodology enables accurate prediction of fertilization schedules, ensuring optimal npk levels for companion planting. This innovation highlights the model's ability to enhance agricultural sustainability and productivity.

However, this study has several limitations. Firstly, the computational costs and data requirements for implementing local antimagic $\boldsymbol{b}-$coloring in large-scale agricultural settings needs further optimization. Secondly, the model's performance in diverse environmental conditions requires additional validation. Future research should focus on refining these parameters and exploring broader applications of the proposed theorems in other domains, such as logistics and network optimization.

Overall, this research bridges theoretical graph concepts with real-world applications, laying a foundation for advanced techniques in precision agriculture and beyond.

ACKNOWLEDGMENTS

We would like to thank all parties involved in the completion of this article, especially PUI-PT Combinatorics and Graphs and LP2M University of Jember for their support in funding this article to be published in a reputable international journal in 2025.

REFERENCES

[1]. Arumugam, S., Premalatha, K., Bača, M., & Semaničová-Feňovčíková, A. (2017). Local antimagic vertex coloring of a graph. Graphs and combinatorics, 33, 275-285.

[2]. Haslegrave, J. (2018). Proof of a local antimagic conjecture. Discrete mathematics & theoretical computer science, 20 (Graph Theory).

[3]. Agustin, I. H., & Kurniawati, E. Y. (2020, May). The upper bound of vertex local antimagic edge labeling on graph operations. In Journal of Physics: Conference Series (Vol. 1538, No. 1, p. 012019). IOP Publishing.

[4]. Nazula, N. H., Slamin, S., & Dafik, D. (2018). Local antimagic vertex coloring of unicyclic graphs. Indonesian Journal of Combinatorics, **2** (1), 30-34.

[5]. Agustin, I. H., & Kurniawati, E. Y. (2020, May). On the local antimagic vertex coloring of sub-devided some special graph. In Journal of Physics: Conference Series (Vol. 1538, No. 1, p. 012021). IOP Publishing.

[6]. Kurniawati, E. Y., & Agustin, I. H. (2019, August). The local antimagic total vertex coloring of graphs with homogeneous pendant vertex. In Journal of Physics: Conference Series (Vol. 1306, No. 1, p. 012047). IOP Publishing.

[7]. Jakovac, M., & Klavžar, S. (2010). The b-chromatic number of cubic graphs. Graphs and Combinatorics, 26, 107-118.
[8]. Irving, R. W., & Manlove, D. F. (1999). The b-chromatic number of a graph. Discrete Applied Mathematics, **91** (1-3), 127-141.
[9]. Javadi, R., & Omoomi, B. (2009). On b-coloring of the Kneser graphs. Discrete Mathematics, **309** (13), 4399-4408.
[10]. Javadi, R., & Omoomi, B. (2012). On b-coloring of cartesian product of graphs. Ars Comb., 107, 521-536.
[11]. Kok, J., & Sudev, N. K. (2016). The b-chromatic number of certain graphs and digraphs. Journal of discrete mathematical sciences and cryptography, **19** (2), 435-445.
[12]. Immanuel, T., & Gella, F. S. (2014). The b-chromatic number of bistar graph. Applied Mathematical Sciences, **8** (116), 5795-5800.
[13]. Ansari, N., Chandel, R. S., & Jamal, R. (2018). On b-chromatic Number of Prism Graph Families. Applications and Applied Mathematics: An International Journal (AAM), **13** (1), 20.
[14]. Effantin, B., & Kheddouci, H. (2003). The b-chromatic number of power graphs. Discrete Mathematics & Theoretical Computer Science, 6.
[15]. Kaliraj, K., & Manjula, M. (2021). b-CHROMATIC NUMBER OF LEXICOGRAPHIC PRODUCT OF SOME GRAPHS. Palestine Journal of Mathematics, 10, 110-121.
[16]. Vernold, V. J., & Venkatachalam, M. (2010). The b-chromatic number of star graph families. Le Matematiche, **65** (1), 119-125.
[17]. Nagarathinam, R., & Parvathi, N. (2020, November). On b-coloring line, middle and total graph of tadpole graph. In AIP Conference Proceedings (Vol. 2277, No. 1). AIP Publishing.
[18]. Jeeva, A., Selvakumar, R., & Nalliah, M. (2017, November). The b-chromatic number of some special families of graphs. In IOP Conference Series: Materials Science and Engineering (Vol. 263, No. 4, p. 042113). IOP Publishing.
[19]. Vernold Vivin, J., & Mohanapriya, N. (2016). On b-chromatic number of some line, middle and total graph families. Mathematical Combinatorics, 1, 116-125.
[20]. Lisna, P. C., & Sunitha, M. S. (2016). The b-chromatic number of Mycielskian of some graphs. International Journal of Convergence Computing, **2** (1), 23-40.
[21]. Xavier, D. F. (2014). b-Chromatic Number of Line Graphs of Certain Snake Graphs. International Journal of Computing Algorithm, 3, 700-703.
[22]. Maitra, S., Palai, J. B., Manasa, P., & Kumar, D. P. (2019). Potential of intercropping system in sustaining crop productivity. International Journal of Agriculture, Environment and Biotechnology, **12** (1), 39-45.
[23]. Gamboa, C. H., Vezzani, F. M., Kaschuk, G., Favaretto, N., Cobos, J. Y. G., & da Costa, G. A. (2020). Soil-root dynamics in maize-beans-eggplant intercropping system under organic management in a subtropical region. Journal of Soil Science and Plant Nutrition, **20** (3), 1480-1490.
[24]. Xu, Q., Xiong, K., Chi, Y., & Song, S. (2021). Effects of crop and grass intercropping on the soil environment in the karst area. Sustainability, **13** (10), 5484.
[25]. Chamkhi, I., Cheto, S., Geistlinger, J., Zeroual, Y., Kouisni, L., Bargaz, A., & Ghoulam, C. (2022). Legume-based intercropping systems promote beneficial rhizobacterial community and crop yield under stressing conditions. Industrial Crops and Products, 183, 114958.
[26]. Weih, M., Mínguez, M. I., & Tavoletti, S. (2022). Intercropping systems for sustainable agriculture. Agriculture, **12** (2), 291.

[27]. You, J., Ying, Z., & Leskovec, J. (2020). Design space for graph neural networks. Advances in Neural Information Processing Systems, 33, 17009-17021.
[28]. Ying, Z., Bourgeois, D., You, J., Zitnik, M., & Leskovec, J. (2019). Gnnexplainer: Generating explanations for graph neural networks. Advances in neural information processing systems, 32.
[29]. Liu, Y., Chen, C., Liu, Y., Zhang, X., & Xie, S. (2021, December). Multi-objective explanations of GNN predictions. In 2021 IEEE International Conference on Data Mining (ICDM) (pp. 409-418). IEEE.
[30]. Agustin, I. H., Hasan, M., Adawiyah, R., Alfarisi, R., & Wardani, D. A. R. (2018, May). On the Locating Edge Domination Number of Comb Product of Graphs. In Journal of physics: conference series (Vol. 1022, No. 1, p. 012003). IOP Publishing.
[31]. Gembong, A. W., & Agustin, I. H. (2017, June). Bound of distance domination number of graph and edge comb product graph. In Journal of Physics: Conference Series (Vol. 855, No. 1, p. 012014). IOP Publishing.
[32]. Hewamalage, H., Bergmeir, C., & Bandara, K. (2021). Recurrent neural networks for time series forecasting: Current status and future directions. International Journal of Forecasting, **37** (1), 388-427.
[33]. Madan, R., & Mangipudi, P. S. (2018, August). Predicting computer network traffic: a time series forecasting approach using DWT, ARIMA and RNN. In 2018 Eleventh International Conference on Contemporary Computing (IC3) (pp. 1-5). IEEE.
[34]. Yunpeng, L., Di, H., Junpeng, B., & Yong, Q. (2017, November). Multi-step ahead time series forecasting for different data patterns based on LSTM recurrent neural network. In 2017 14th web information systems and applications conference (WISA) (pp. 305-310). IEEE.
[35]. Agustin I H, Dafik, Hasan M, Alfarisi R, and Prihandini R M. 2017. Local Edge Antimagic Coloring of Graphs. *Far East Journal of Mathematical Sciences*. Volume 102, Number 9, Pages 1925-1941.
[36]. Slamin, S., Adiwijaya, N. O., Hasan, M. A., Dafik, D., & Wijaya, K. (2020). Local super antimagic total labeling for vertex coloring of graphs. Symmetry, **12** (11), 1843.
[37]. Lau, G. C., Ng, H. K., & Shiu, W. C. (2020). Affirmative solutions on local antimagic chromatic number. Graphs and combinatorics, **36** (5), 1337-1354.
[38]. Melo, R. A., Queiroz, M. F., & Santos, M. C. (2021). A matheuristic approach for the b-coloring problem using integer programming and a multi-start multi-greedy randomized metaheuristic. European Journal of Operational Research, **295** (1), 66-81.
[39]. Jaffke L, Lima P T, and Lokshtanov D. 2023. b −Coloring parameterized by clique-width. Theory of *Computing Systems*, 1-33.
[40]. Lim, B., & Zohren, S. (2021). Time-series forecasting with deep learning: a survey. Philosophical Transactions of the Royal Society A, **379** (2194), 20200209.
[41]. Jiang, W., & Luo, J. (2022). Graph neural network for traffic forecasting: A survey. Expert systems with applications, 207, 117921.
[42]. Wu, S., Sun, F., Zhang, W., Xie, X., & Cui, B. (2022). Graph neural networks in recommender systems: a survey. ACM Computing Surveys, **55** (5), 1-37.
[43]. Septory, B.J., Utoyo, M.I., Sulistiyono, B. and Agustin, I.H. 2021. On rainbow antimagic coloring of special graphs. In Journal of Physics: Conference Series (Vol. 1836, No. 1, p. 012016). IOP Publishing.
[44]. Dafik, Agustin, I.H., Surahmat, Alfarisi, R., and Sy, S. 2017. on Non-Isolated Resolving Number of Special Graphs and Their Operations. Far East Journal of Mathematical Sciences, 102, 2473-2492.

[45]. Alfarisi, R., Prihandini, R.M., Adawiyah, R., Albirri, E.R. and Agustin, I.H., 2019. Graceful chromatic number of unicyclic graphs. Journal of Physics: Conference Series (Vol. 1306, No. 1, p. 012039). IOP Publishing.